Influence of the crystalline microstructure on the magnetic ordering of nanocrystalline chromium

D. Wardecki and R. Przeniosło
Institute of Experimental Physics, University of Warsaw, Hoża 69, 00-681 Warsaw, Poland

M. Bukowski and R. Hempelmann
Institute of Physical Chemistry, University of Saarbrücken, D66123 Saarbrücken, Germany

A. N. Fitch
European Synchrotron Radiation Facility, F-38042 Grenoble Cedex, France

P. Convert
Institute Laue-Langevin, Boîte Postale 220, F-38043 Grenoble Cedex, France

(Received 6 June 2012; revised manuscript received 11 July 2012; published 6 August 2012)

The magnetic and structural properties of nanocrystalline chromium (n-Cr) were studied by neutron powder diffraction and by synchrotron radiation diffraction techniques. The nanocrystalline Cr is composed of small-sized particles with antiferromagnetic ordering, medium-sized particles with transverse spin density wave (SDW) ordering, and large-sized particles with the same magnetic ordering as bulk Cr. The critical size D_C between the small and medium-sized crystallites is 18 ± 2 nm. The alteration of the magnetic properties of n-Cr is due to microstrain fluctuations which are correlated with the crystallite sizes rather than to the crystallite size itself. The microstrain fluctuations increase the SDW modulation length up to large values (10.5 nm for n-Cr vs 7.8 nm for bulk Cr).

DOI: 10.1103/PhysRevB.86.064410 PACS number(s): 75.75.−c, 61.05.cp, 61.05.fm, 61.72.−y

I. INTRODUCTION

Chromium is an important model system with complex magnetic properties.[1] The crystal structure of bulk Cr is a cubic bcc-type while the magnetic ordering is antiferromagnetic superimposed on a spin density wave (SDW) modulation with the modulation length Λ_{SDW} varying with temperature between 6.0 and 7.8 nm.[2] It is interesting to study the magnetic properties of chromium in nanocrystalline form,[3,4] especially because the crystallite sizes are a few times larger than the modulation length Λ_{SDW}, i.e., about 25–75 nm. This question has already been addressed in many neutron and/or x-ray diffraction studies performed with strained Cr polycrystals,[5,6] Cr nanocrystals,[7–10] and epitaxial Cr thin films.[11–13] In the present paper we describe a combined approach using neutron powder diffraction and high resolution synchrotron radiation (SR) diffraction which show the influence of the crystalline microstructure on the magnetic ordering of electrodeposited nanocrystalline Cr.[10,14,15] We show important alterations of the magnetic ordering in n-Cr mainly due to the microstructure and we describe a method which combines the analysis of both neutron and SR diffraction data with one common model.

II. EXPERIMENT

The samples of nanocrystalline chromium were prepared by the electrodeposition method proposed by Tsai and Wu.[16] This paper describes studies of three samples: n-Cr2 (29 nm), n-Cr3 (31 nm), and n-Cr4 (65 nm), which were prepared earlier as discussed in Ref. 15. The size given next to the sample label represents the volume averaged crystallite size as described in Ref. 15. The first two samples, i.e., n-Cr2 (29 nm) and n-Cr3 (31 nm) were used in the "as-prepared" form while the sample n-Cr4 (65 nm) was annealed in air at 500 °C for 25 min in order to increase its crystallite sizes. A reference polycrystalline commercial chromium sample (poly-Cr) from Goodfellow was also used. The crystalline microstructure of n-Cr samples has been characterized by using the high-resolution synchrotron radiation diffraction method on the beamline ID-31 at ESRF[17] operating at the wavelength 0.39988(4) Å.[15]

Neutron powder diffraction was used to study the magnetic ordering of n-Cr. The measurements were performed by using the high flux neutron diffractometer D20 at ILL[18] operating at the neutron wavelength $\lambda = 1.292$ Å. The n-Cr and poly-Cr samples of powder form were enclosed in vanadium containers and placed in an orange cryostat. The measurements were performed by slow cooling between 310 K and 4 K. The contribution due to neutrons with $\lambda/2$ wavelength was observed to be about 0.26% of the primary beam intensity. The estimated $(\lambda/2)$ contribution was subtracted from the measured neutron powder diffraction patterns.

The crystal structure of all the n-Cr samples in this study is a cubic bcc-type as for bulk Cr[1] in agreement with earlier results.[10,15] The crystallite size distribution and the microstrain have been determined from SR diffraction data by using the Warren-Averbach[19] method assuming spherical crystallites with a log-normal distribution of the crystallite sizes as described in Ref. 20. The calculations were performed by using the program GADGET.[21,22]

III. RESULTS

The grain growth process in annealed n-Cr leads to larger crystallite sizes and reduces the microstrain fluctuations $\Delta d/d$. Our earlier studies[15,21] have shown a saturation of crystallite size growth and microstrain changes in n-Cr at annealing times longer than 30 min. The dependence among the final

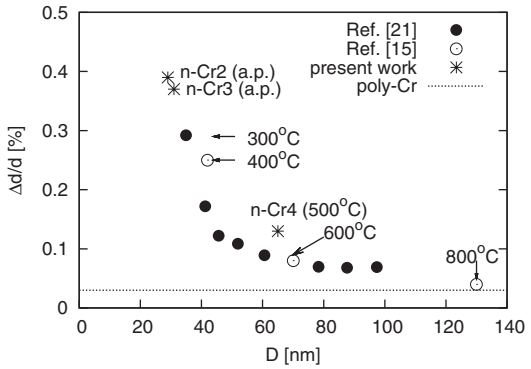

FIG. 1. Dependence between the microstrain fluctuations $\Delta d/d$, the average crystallite size D, and the annealing temperature for electrodeposited nanocrystalline chromium. The solid and empty symbols are taken from Refs. 15 and 21, respectively, while the star symbols denote the samples studied in the present paper. The dotted line represents the microstrain fluctuations observed in standard poly-Cr. The samples n-Cr2 and n-Cr3 were used in "as prepared" (a.p.) form while n-Cr4 was annealed at 500 °C.

microstrain fluctuations $\Delta d/d$, the final average crystallite size, and the annealing temperature is shown in Fig. 1. The points corresponding to the as-prepared samples n-Cr2 (29 nm), n-Cr3 (31 nm) and the annealed sample n-Cr4 (65 nm) are labeled in Fig. 1. The microstrain fluctuation parameters determined for n-Cr samples used in this study are given in Table I. The microstructural parameters of annealed n-Cr samples described by Ishibashi *et al.*[7] and epitaxial Cr films described by Sonntag *et al.*[11] are also given in Table I. The microstrain fluctuations for annealed n-Cr were not given in the paper by Ishibashi *et al.*[7] The limitation $\Delta d/d < 0.03\%$ is concluded from our present data shown in Fig. 1. The correlation between the average crystallite size and the microstrain fluctuation is discussed in the context of the magnetic properties of n-Cr in the next paragraphs.

There are three main magnetic orderings reported for chromium: the collinear antiferromagnetic phase (AF_0) and two modulated phases: transversal TSDW (referred to as AF_1) and longitudinal LSDW (referred to as AF_2).[1] A schematic representation of these orderings and their contributions to the neutron powder diffraction patterns in the region around the (1,0,0) Bragg position are explained in Bacon and Cowlam.[6] In the powder diffraction method both AF_0 and AF_2 phases contribute only to the (1,0,0) Bragg peak position while the AF_1 phase contributes also to the satellite peaks: $(1+\delta,0,0)$ and $(1-\delta,0,0)$.

TABLE I. Surface and volume averaged crystallite size, $\langle L\rangle_s$, $\langle L\rangle_v$, and microstrain fluctuations $\Delta d/d$ obtained for the n-Cr samples and the standard poly-Cr sample. Literature results for annealed n-Cr[7] and epitaxial Cr films[11] are shown.

Sample	$\langle L\rangle_s$ (nm)	$\langle L\rangle_v$ (nm)	$\Delta d/d$ (%)
n-Cr2 (29 nm)	23(1)	29(1)	0.39(1)
n-Cr3 (31 nm)	27(1)	31(2)	0.37(4)
n-Cr4 (65 nm)	42(1)	65(3)	0.13(1)
poly-Cr	55(2)	105(2)	0.03(1)
n-Cr[7]	Annealed	100	<0.03
Epitaxial Cr[11]	Film thickness	100	0.26

The observed neutron powder diffraction patterns were analyzed by the Rietveld method assuming the bcc-type crystal structure of Cr. There is no correlation between the lattice parameter at RT and the average crystallite size, i.e., all n-Cr samples gave lattice parameters very close to the bulk Cr reference values. The anomalies of the n-Cr lattice parameters reported earlier in Ref. 10 could not be detected in the present studies. The region of the neutron diffraction pattern around the magnetic peaks around the (1,0,0) position have been refined by assuming three Gaussian functions (with the same widths) representing the $(1-\delta,0,0)$, (1,0,0), and $(1+\delta,0,0)$ peaks plus a linear background. The magnetic peak located at (1,0,0) has the same full width at half maximum as the nearest Bragg peak (1,1,0) due to the *bcc* crystal structure of Cr. The observed intensities were used to calculate the amount of the AF_0 and AF_1 magnetic phases. The magnetic form factor for Cr^{2+} tabulated in the *International Tables for Crystallography*,[23] which has almost the same values as the magnetic form factor for metallic Cr determined by Freeman and Watson,[24] was used in the calculations. The SDW amplitude of $M_0 = 0.59\mu_B$ of the AF_1 phase was assumed to be constant in the whole temperature range. This value is taken from studies of bulk Cr at T = 78 K by Shirane and Takei.[25] With these two assumptions and the result of the Rietveld analysis of the crystal structure it is possible to estimate the amount of AF_1 and AF_0 phases and also the value of the ordered magnetic moments per one Cr atom for the AF_0 phase. The resulting temperature dependences of the AF_1 and AF_0 phases' relative volumes obtained for n-Cr and poly-Cr are shown in Fig. 2. The characteristic parameters of the AF_0 and AF_1 magnetic phases obtained at 130 K for n-Cr and poly-Cr are given in Table II.

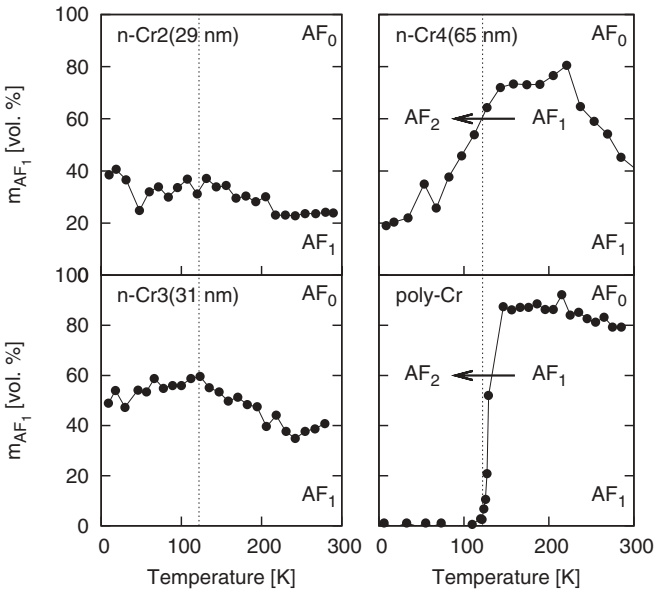

FIG. 2. Temperature changes of the relative volume m_{AF_1} occupied by the AF_1 magnetic phase for n-Cr and poly-Cr samples. The arrows indicate possible spin-flip ($AF_1 \rightarrow AF_2$) transitions. Vertical dotted lines indicate the spin-flip temperature $T_{SF} = 122$ K observed for bulk Cr.[1]

TABLE II. Results of neutron diffraction studies of nanocrystalline Cr and polycrystalline Cr at $T = 130$ K. The relative volume occupied by the antiferromagnetic AF_0 (m_{AF_0}) and the modulated AF_1 phase (m_{AF_1}) is given together with the value of the ordered magnetic moment per one Cr atom in the AF_0 phase.

Sample	m_{AF_0} (vol. %)	m_{AF_1} (vol. %)	μ (AF_0) (μ_B/atom)
n-Cr2 (29 nm)	65(2)	35(2)	0.60(3)
n-Cr3 (31 nm)	43(2)	57(2)	0.42(3)
n-Cr4 (65 nm)	27(2)	73(2)	0.36(3)
poly-Cr	13(1)	87(1)	0.40(3)

The reference poly-Cr sample shows a sharp spin-flip transition at $T_{SF} = 122$ K in agreement with bulk Cr properties.[1] In the n-Cr4 (65 nm) sample with larger average crystallite sizes a part of the volume shows a smeared spin-flip transition below 122 K. In the n-Cr2 (29 nm) and n-Cr3 (31 nm) samples with smaller crystallite sizes the spin-flip transition is almost completely suppressed and a large part of the volume remains in the AF_1 phase at low temperatures down to 4 K.

The neutron diffraction data has been also used to determine the SDW modulation length Λ_{SDW} as shown in Fig. 3. The poly-Cr gives the same Λ_{SDW} values as the literature reference bulk Cr[2] while the nCr2 (29 nm) and nCr4 (65 nm) samples show a systematic increase of Λ_{SDW} in the whole temperature range. The reported Λ_{SDW} have been determined from magnetic satellite peak positions $(1 + \delta,0,0)$ and $(1 - \delta,0,0)$ in the neutron diffraction patterns. The microstrain fluctuations $\Delta d/d$ have been determined from the widths of Bragg peaks in the SR based x-ray diffraction patterns. Both Λ_{SDW} and $\Delta d/d$ are average values determined for each sample. It is not possible to obtain more detailed information about possible changes of the magnetic modulations and/or microstrain fluctuations in different regions of the same nanosized crystallite. The increase of Λ_{SDW} is largest for samples with the smallest crystallite sizes. The largest Λ_{SDW} values obtained for the n-Cr2 (29 nm) sample are compared with the available literature data for nanocrystalline Cr in Fig. 3. An annealed nanocrystalline Cr sample with an average crystallite size of 100 nm studied with neutron diffraction by Ishibashi *et al.*[7] shows the same $\Lambda_{SDW}(T)$ as bulk Cr[2] (see Fig. 3). On the other hand, epitaxial Cr films with 100-nm thickness were studied with SR based x-ray diffraction by Sonntag *et al.*[11] The results given in Ref. 11 concern the strain wave (SW)/charge density wave (CDW) in Cr which contributes to $(2 \pm 2\delta,0,0)$ satellite peaks in x-ray diffraction giving information about the CDW modulation length Λ_{CDW}. The values of the magnetic SDW modulation length shown in Fig. 3 were calculated as $\Lambda_{SDW} = 2\Lambda_{CDW}$ according to Refs. 11 and 26. The Λ_{SDW} values for Cr films[11] show also a systematic increase as compared with bulk Cr values.[2]

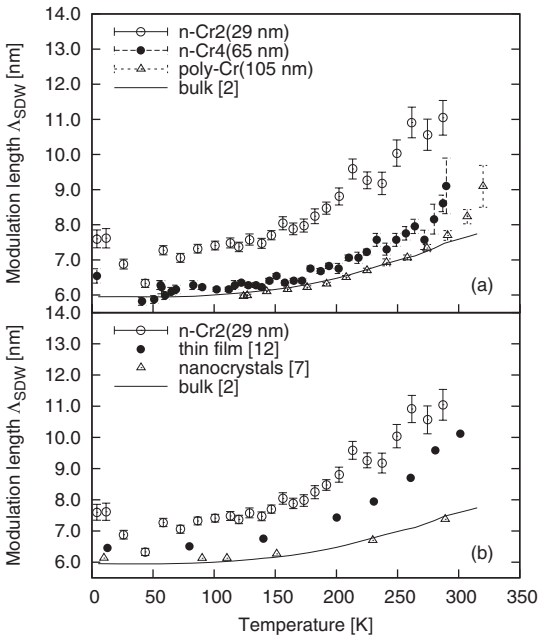

FIG. 3. (a) Temperature changes of the modulation length Λ_{SDW} for n-Cr, poly-Cr, and reference bulk Cr.[2] (b) Temperature changes of the modulation length Λ_{SDW} for n-Cr, Cr thin film (100 nm),[12] and annealed n-Cr (100 nm).[7]

The effects of increase of Λ_{SDW} observed in Fig. 3 are most probably due to the microstrain fluctuations rather than to the crystallite sizes. This assumption can explain the almost vanishing increase of Λ_{SDW} observed in annealed n-Cr[7] (100-nm size) and the large increase observed in epitaxial Cr films[11] (of the same thickness, i.e., 100 nm). The relation between the Λ_{SDW} increase and the microstrain fluctuations increase is in agreement with our present data (see Fig. 3 and Table I). It is also in agreement with the results for epitaxial Cr films with different thicknesses and strains presented in Ref. 11.

The increase of Λ_{SDW} shown in Fig. 3 and reported by other authors[7,11] should be compared with literature data on the influence of doping and external pressure on the SDW ordering in chromium. The external pressure decreases the Λ_{SDW} in Cr single crystals[27,28] and it is contrary to our observations for n-Cr shown in Fig. 3 and given by other authors.[7,11] Another way to change the Λ_{SDW} is doping which works in two ways. Doping with acceptors decreases the Λ_{SDW} as shown, e.g., for Cr-V and Cr-Ta,[29] while doping with donors increases the Λ_{SDW}, e.g., for Cr-Mn and Cr-Re.[29]

In the present case of n-Cr there was no doping but one could expect possible effects of the pressure due to microstrain fluctuations in the SDW ordering. For isolated nanosized metallic particles one can expect a contraction of the interatomic distances in the surface region as compared with the particle interior as observed for Al.[30] The n-Cr samples studied in the present paper are not isolated but agglomerated in the electrodeposition process as shown in scanning electron microscopy micrographs, see Fig. 4 in Ref. 15. It is not clear what the morphology of the particle boundary regions is and it is not known for sure if the interatomic distance contraction mechanism observed in isolated Al (Ref. 30) can be applied to the present case of n-Cr.

The temperature dependence of Λ_{SDW} observed for n-Cr samples has a similar shape and it is shifted *upwards* as compared with that for reference poly-Cr (see Fig. 3). A very similar image has been observed in pressure studies[27] where the temperature dependence of Λ_{SDW} observed under pressure has a similar shape and it is shifted *downwards* as compared with that for ambient pressure.

The results for n-Cr shown in Fig. 3 might fit to the image given in Ref. 27 with negative pressures. This interpretation may not be realistic and other mechanisms could decide. It is also possible that the Fermi surface in n-Cr has deformations different from those in the single crystals due to limited size and the influence of strained grain boundaries. The question on the reason for the Λ_{SDW} increase in n-Cr is still open.

The influence of the crystalline microstructure on the observed magnetic properties of n-Cr can be described by using the model proposed in Ref. 7 which assumes three categories of crystallites in chromium:

(1) small-sized crystallites which have only the AF_0 magnetic phase,

(2) middle-sized crystallites which have the AF_1 magnetic phase down to the lowest temperature (i.e., no spin-flip transition),

(3) large-sized crystallites which have the same magnetic ordering as bulk Cr, i.e., AF_1 above $T_{SF} = 122$ K and AF_2 below T_{SF}.

This model can be applied quantitatively to the n-Cr samples used in the present paper. The relative volume occupied by the AF_0 phase is known from neutron diffraction data (see Table II) while the crystallite size distribution is known from SR diffraction data. The log-normal distribution describing the crystallite size D in a sample has the following form:

$$f(D) = \frac{1}{\sqrt{2\pi}\, D \ln\sigma} \exp\left\{-\frac{1}{2}\left(\frac{\ln(D/\mu)}{\ln\sigma}\right)^2\right\}, \qquad (1)$$

where μ and σ are parameters of the distribution which were determined for all n-Cr samples in the present paper. The values of μ and σ are given in Table III.

Assuming that the small-sized crystallites with diameters below some critical value of D_C have only the AF_0 phase one can calculate what is the relative volume occupied by these small crystallites. One needs to transform the distribution of crystallite diameters $f(D)$ into the distribution of volumes $g(V)$:

$$g(V) = f[D(V)]\left|\frac{dD}{dV}\right|, \qquad (2)$$

where for spherical crystallites

$$D(V) = (6V/\pi)^{\frac{1}{3}}. \qquad (3)$$

The cumulative distribution function $G(V)$ is defined as

$$G(V) = \int_0^V g(V')dV'. \qquad (4)$$

TABLE III. The parameters of the distribution $f(D)$ as well as the critical size D_C for n-Cr and poly-Cr samples.

Sample	μ (nm)	σ	m_{AF_0} (%)	D_C (nm)
n-Cr2 (29 nm)	15.3	1.68	65(2)	18(1)
n-Cr3 (31 nm)	17.8	1.63	43(2)	16(1)
n-Cr4 (65 nm)	28.5	1.76	27(2)	20(1)
poly-Cr	22.2	2.07	13(1)	9(1)

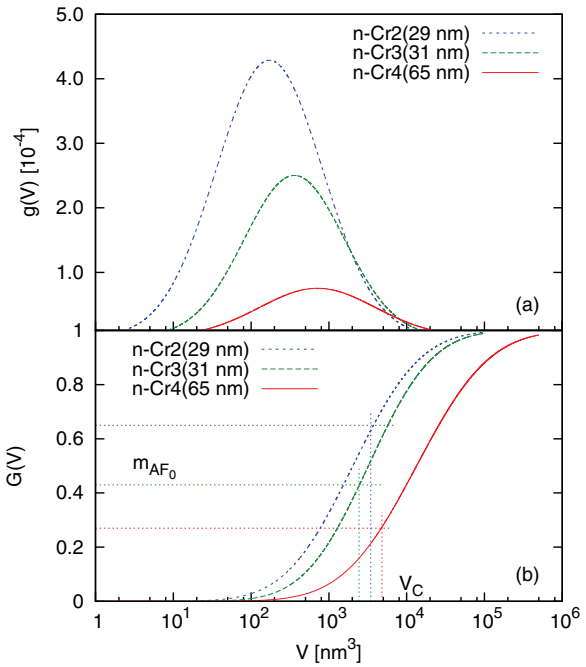

FIG. 4. (Color online) Log-normal distribution function $g(V)$ (a) and the cumulative distribution function $G(V)$ (b) for the n-Cr samples. The vertical dotted lines (b) indicate the critical volumes V_C while the horizontal dotted lines denote the relative volume m_{AF_0} of the AF_0 magnetic phase determined for n-Cr at 130 K (see Table II).

The distribution functions $g(V)$ as well as the cumulative distribution functions $G(V)$ for the n-Cr samples are shown in Fig. 4. One can determine the critical volume V_C as

$$G(V_C) = m_{AF_0}, \qquad (5)$$

where m_{AF_0} is the relative volume occupied by the AF_0 phase. From the value of V_C one can calculate the critical diameter D_C by using Eq. (3). The values of the critical crystallite diameters D_C vary between 16 and 20 nm for all the n-Cr samples as shown in Table III.

IV. CONCLUSIONS

We may conclude that the model description assuming small, medium, and large Cr crystallites with different magnetic properties as proposed by Ishibashi *et al.*[7] agrees well with our observations and the critical size is $D_C = 18 \pm 2$ nm. Earlier studies by Ishibashi *et al.*[7] and Tsunoda *et al.*[8] gave a limit of 13–15 nm for small crystallites with pure antiferromagnetic ordering.

ACKNOWLEDGMENTS

Thanks are due to colleagues from the Condensed Matter Structure Laboratory at the University of Warsaw for discussion. One of the authors (D.W.) thanks the ESRF for support during his stay. The access to the ILL and ESRF facilities has been supported by the Ministry of Science and Higher Education (Poland) under Projects No. 458/1/N-ILL/2010/0 and No. 155/ESR/2006/03, respectively.

[1]E. Fawcett, Rev. Mod. Phys. **60**, 209 (1988).
[2]S. Werner, A. Arrott, and H. Kendrick, Phys. Rev. **155**, 528 (1967).
[3]H. Gleiter, Prog. Mater. Sci. **33**, 223 (1989).
[4]E. Roduner, *Nanoscopic Materials: Size-Dependent Phenomena* (Royal Society of Chemistry Publishing, Cambridge, 2006).
[5]G. Bacon, Acta Crystallogr. **14**, 823 (1961).
[6]G. Bacon and N. Cowlam, J. Phys. C **2**, 238 (1969).
[7]H. Ishibashi, K. Nakahigashi, and Y. Tsunoda, J. Phys.: Condens. Matter **5**, L415 (1993).
[8]Y. Tsunoda, H. Nakano, and S. Matsuo, J. Phys.: Condens. Matter **5**, L29 (1993).
[9]M. R. Fitzsimmons, J. A. Eastman, R. A. Robinson, A. C. Lawson, J. D. Thompson, R. Movshovich, and J. Satti, Phys. Rev. B **48**, 8245 (1993).
[10]R. Przeniosło, I. Sosnowska, G. Rousse, and R. Hempelmann, Phys. Rev. B **66**, 014404 (2002).
[11]P. Sonntag, P. Bödeker, A. Schreyer, H. Zabel, and K. H. H. Kaiser, J. Magn. Magn. Mater. **183**, 5 (1998).
[12]P. Sonntag, P. Bödeker, T. Thurston, and H. Zabel, Phys. Rev. B **52**, 7363 (1995).
[13]H. Zabel, J. Phys.: Condens. Matter **11**, 9303 (1999).
[14]R. Przeniosło, J. Wagner, H. Natter, R. Hempelmann, and W. Wagner, J. Alloys Comp. **328**, 259 (2001).
[15]D. Wardecki, R. Przeniosło, A. Fitch, and M. Bukowski, J. Nanopart. Res. **13**, 1151 (2011).
[16]R. Tsai and S. Wu, J. Electrochem. Soc. **137**, 3057 (1990).
[17]A. Fitch, J. Res. Natl. Inst. Stand. Technol. **109**, 133 (2004).
[18]P. Convert, T. Hansen, and J. Torregrossa, Mater. Sci. Forum **321–324**, 314 (2000).
[19]B. Warren and B. Averbach, J. App. Phys. **21**, 595 (1950).
[20]C. Krill and R. Birringer, Philos. Mag. A **77**, 621 (1998).
[21]G. Chojnowski, R. Przeniosło, I. Sosnowska, M. Bukowski, H. Natter, R. Hempelmann, A. Fitch, and V. Urban, J. Phys. Chem. C **111**, 5599 (2007).
[22]G. Chojnowski, M.Sc. thesis, Faculty of Physics, University of Warsaw, 2004.
[23]A. Wilson, *International Tables for Crystallography* (International Union of Crystallography, Kluwer Academic, Dordrecht, 1995).
[24]A. Freeman and R. Watson, Acta Crystallogr. **14**, 231 (1961).
[25]G. Shirane and W. J. Takei, J. Phys. Soc. Jpn. Suppl. B-III **17**, 35 (1962).
[26]Y. Tsunoda, M. Mori, N. Kunitomi, Y. Teraoka, and J. Kanamori, Solid State Commun. **14**, 287 (1974).
[27]H. Umebayashi, G. Shirane, and B. Frazer, J. Phys. Soc. Jpn. **24**, 368 (1968).
[28]Y. Feng, R. Jaramillo, G. Srajer, J. C. Lang, Z. Islam, M. S. Somayazulu, O. G. Shpyrko, J. J. Pluth, H.-k. Mao, E. D. Isaacs, G. Aeppli, and T. F. Rosenbaum, Phys. Rev. Lett. **99**, 137201 (2007).
[29]R. Griessen and E. Fawcett, Phys. B **91**, 205 (1977).
[30]J. Woltersdorf, A. Nepijko, and E. Pippel, Surf. Sci. **106**, 64 (1981).